

Cite this article as: Shang Fangjing, Wang Wenxian, Yang Tao, et al. Interaction Mechanism and Wear Resistance of Ni-encapsulated Al_2O_3 Particles Reinforced Iron Matrix Composites[J]. Rare Metal Materials and Engineering, 2022, 51(02): 422-428.

ARTICLE

Interaction Mechanism and Wear Resistance of Ni-encapsulated Al_2O_3 Particles Reinforced Iron Matrix Composites

Shang Fangjing¹, Wang Wenxian¹, Yang Tao², Liu Ruihong³, Zhou Jun⁴

¹College of Materials Science and Engineering, Taiyuan University of Technology, Taiyuan 030024, China; ²College of Mechanical Engineering, Taiyuan University of Technology, Taiyuan 030024, China; ³College of Aeronautics and Astronautics, Taiyuan University of Technology, Taiyuan 030024, China; ⁴Department of Mechanical Engineering, Penn State Erie, The Behrend College, PA 16563, USA

Abstract: Ni coating was prepared on the surface of Al_2O_3 by chemical deposition method. Ni coated Al_2O_3 particles ($\text{Al}_2\text{O}_3\text{p}@\text{Ni}$) was used as particle-reinforcement for iron matrix. The $\text{Al}_2\text{O}_3\text{p}@\text{Ni}/\text{Fe}$ composites were prepared by SPS. Results show that by optimizing electroless plating process, the surface of Al_2O_3 is uniformly covered by Ni. Ni coating presents a typical cauliflower structure with the size of 1~4 μm , which is deposited in pits and holes on the surface of Al_2O_3 and then gradually extends outwardly. The thickness of Ni layer is up to 100.55 μm , and Ni coating is closely bounded to Al_2O_3 . In the process of sintering, Ni coatings not only improve the wettability between Al_2O_3 and iron matrix, but also promote the diffusion and reaction of Al_2O_3 and iron matrix at the interface. Finally, $\text{Al}_2\text{O}_3/\text{NiAl}_2\text{O}_4/(\text{Al}_{0.8}\text{Cr}_{0.2})_2\text{O}_3/\text{NiFe}_2\text{O}_4/\text{Ni}/\text{iron}$ matrix interface layer is formed by mechanical bonding, interdiffusion and chemical reactions, which can improve interface bonding strength greatly. The wear tests of $\text{Al}_2\text{O}_3\text{p}@\text{Ni}/\text{Fe}$ composites and $\text{Al}_2\text{O}_3\text{p}/\text{Fe}$ composites were carried out. Compared with $\text{Al}_2\text{O}_3\text{p}/\text{Fe}$ composites, the wear mass loss of $\text{Al}_2\text{O}_3\text{p}@\text{Ni}/\text{Fe}$ composites is decreased by 50%, and the friction coefficient is decreased by 12.5%. The wear resistance of $\text{Al}_2\text{O}_3\text{p}@\text{Ni}/\text{Fe}$ composites is greatly improved.

Key words: electroless plating; $\text{Al}_2\text{O}_3@\text{Ni}/\text{Fe}$ composites; SPS; wear resistance

Ceramic particles reinforced metal matrix composites (MMCs) have become a research hotspot due to their high hardness, high temperature strength and good wear resistance. And ceramic particles reinforced iron matrix composites have become a new trend to fabricate wear resistant materials instead of iron and steel.

Different from traditional smelting method, which may have segregation and porosity defects, powder metallurgy method is the main method for the fabrication of high-content ceramic-reinforced metal matrix composites. Fan et al^[1] fabricated alumina particles reinforced iron matrix composites by powder metallurgy. And they found out that by adding element C, the microstructure of matrix changes from ferrite to ferrite and pearlite, the hardness increases significantly which can reach about 9000 MPa, and the wear resistance improves significantly. Dang et al^[2] fabricated $\text{Al}_2\text{O}_3/\text{Cu}$

composites by near melting point casting method, and the wear resistance is increased by 36.6% with addition of 0.6wt% La_2O_3 . NASA has fabricated B/Al composite materials by powder metallurgy method, which have been applied to aircraft cargo compartment truss. Toyota has fabricated SiC- Al_2O_3 reinforced aluminum matrix composites by powder metallurgy, which have been applied to wear-resistant piston, and the wear resistance is improved greatly^[3].

However, due to the poor wettability of ceramics and metals, for example, the wetting angle of Al_2O_3 to iron solution is 140°, so it is difficult for ceramics to connect ceramics with metals^[4]. Unlike metals, which are composed of metallic bonds, ceramics are composed of covalent bonds. The different bond types also make it hard to react. Therefore, the bonding strength of the ceramic-metal interface is poor, so the ceramic particles are easy to fall off in service. At present,

Received date: February 18, 2021

Foundation item: National Natural Science Foundation of China (51775366)

Corresponding author: Wang Wenxian, Ph. D., Professor, College of Materials Science and Engineering, Taiyuan University of Technology, Taiyuan 030024, P. R. China, Tel: 0086-351-6010076, E-mail: wangwenxian@tyut.edu.cn

Copyright © 2022, Northwest Institute for Nonferrous Metal Research. Published by Science Press. All rights reserved.

numerous surface modification technologies are used to improve the wettability of ceramic and metal, such as ball-milling, sol and electroless platings. Hong et al^[5] successfully fabricated a homogeneous nickel layer on the surface of zirconia toughened alumina ceramics (ZTA) by electroless plating. Ru et al^[6,7] fabricated uniform and continuous nickel-coated ZTA powder by ionic liquid assisted deposition method. The thickness of Ni coating reaches 7~10 μm . They measured the wettability of molten iron on the surface of nickel-plated zirconia toughened alumina ceramic (ZTA@Ni). The results show that, compared with ZTA without surface treatment, the wetting angle of 65Mn liquid on ZTA@Ni plate decreases from 104.1° to 83.6°, and that of the high chromium cast iron liquid on ZTA@Ni plate decreases from 102.3° to 88.2°. At the same time, they also analyzed the interface behavior of ZTA@Ni reinforced iron matrix composites. At a high casting temperature, Ni diffuses into the iron solution and reacts with Al_2O_3 to generate Al_2NiO_4 . The mutual diffusion of Ni and other elements at the interface between ZTA and iron can enhance the interfacial bonding strength. Olgun et al^[8] successfully coated a ZrB_2 layer with a thickness of 15~20 μm on the surface of copper by ball milling. Guo et al^[9] fabricated ultrafine WC/Co composite powders by electroless plating. The Co layer with an average thickness of 50~100 nm was fabricated on the surface of WC particles with a diameter of 0.3~0.5 μm . Results show that the rate of electroless plating has an exponential relation with temperature, and the coating thickness has a certain relation with pH value. Wang et al^[10] successfully fabricated TiO_2 film on stainless steel surface by plasma Ti-thermal oxidation method.

At present, Al_2O_3 is widely used as reinforcement particles to fabricate ceramic reinforced iron-based wear-resistant materials because of its low price and the possibility to manufacture complex geometry parts. Considering the coating quality, pricing factor and industrializable preparation, electroless plating is an ideal surface treatment method, which has been successfully carried out on the surface of Al_2O_3 ^[11]. Ni is good as an interlayer considering the phenomenon of infinite solution of Ni layer and molten iron, which can greatly improve the wettability between ceramic and metal, and promote the interface connection greatly^[12,13].

In this study, copper ion auxiliary solution was used for pretreatment firstly, Ni coating was fabricated on the surface of Al_2O_3 by chemical deposition method, and sodium hypophosphite was used to reduce nickel ions. The Ni coated Al_2O_3 particle ($\text{Al}_2\text{O}_3@Ni$) was used as the precursor for reinforcing iron matrix composite. The morphology of the Ni coating on the Al_2O_3 surface was observed. Then $\text{Al}_2\text{O}_3@Ni$ reinforced iron matrix composites ($\text{Al}_2\text{O}_3@Ni/\text{Fe}$) was prepared by powder sintering method, and the morphology, phase composition and element distribution of $\text{Al}_2\text{O}_3@Ni/\text{Fe}$ composites were investigated. The interaction mechanism between $\text{Al}_2\text{O}_3@Ni$ and iron matrix was described in combination with the sintering process. In addition, the wear resistance of the composites was

also measured.

1 Experiment

1.1 Chemicals

In this study, 95wt% Al_2O_3 with a diameter of 3 mm was used as the reinforcing particle, purchased from Aladdin, and high-chromium steel was used as the matrix. The composition of high-chromium steel is shown in Table 1.

1.2 Fabrication of Ni-encapsulated Al_2O_3 particles

The preparation of $\text{Al}_2\text{O}_3@Ni$ particles includes pretreatment and electroless plating. Firstly, the Al_2O_3 particles were cleaned, coarsened, sensitized and activated, then soaked in deionized water and cleaned by ultrasonic vibration, and finally the surface with catalytic activity was obtained. The optimal pretreatment process is shown in Table 2.

The pretreated Al_2O_3 particles were pre-plated and placed into the copper ion auxiliary solution for 3 min, and then put into the nickel plating solution for 1 h. The optimal plating solution process is shown in Table 3. The pH of the solution was 5.7, the temperature was 60 °C, and the stirring rate of agitation was 200 r/min. After the electroless plating, the samples were cleaned with deionized water and dried in the drying oven.

1.3 Preparation of $\text{Al}_2\text{O}_3@Ni/\text{Fe}$ composites

$\text{Al}_2\text{O}_3@Ni$ particles and iron matrix were uniformly mixed in a volume ratio of 1:5, and then the mixture was sintered by SPS, and the sintering temperature of 960 °C, the holding time of 10 min and the pressure of 30 MPa were used to fabricate

Table 1 Chemical composition of steel matrix (wt%)

C	Cr	Si	B	Ni	Fe
0.4~1.2	14~20	2.5~3.5	1.2~2.0	10~15	Bal.

Table 2 Composition and content of the chemicals used in pretreatment process

Component	Content	Stage
Acetone	-	Washing
NaOH	20 g/L	Washing
HCl	20 mL/L	Coarsening
SnCl_2	20 g/L	Sensitizer
PdCl_2	0.5 g/L	Activation

Table 3 Chemical composition of electroless plating

Component	Content/ $\text{g}\cdot\text{L}^{-1}$	Role in bath or operating parameters
Ion auxiliary solution (CuSO_4)	10	Main salt
NiCl_2	60	Main salt
NaH_2PO_2	80	Reducing agent
$\text{C}_6\text{H}_5\text{Na}_3\text{O}_7$	48	Complexing agent
$\text{NaKC}_4\text{H}_4\text{O}_6$	144	Buffering agent

$\text{Al}_2\text{O}_3@\text{Ni}/\text{Fe}$ composites.

1.4 Characterization

The distribution of Al_2O_3 particles and the interfacial connection between Al_2O_3 and iron matrix were observed by metallographic microscope (DMC2900 OM). Y-2000 X-ray diffractometer (XRD) was used to analyze the phase at the interface between Al_2O_3 and iron matrix. The microstructure and element distribution at the interface were characterized by scanning electron microscopic (SEM TESCAN MIRA3 LMH). To evaluate the wear resistance of $\text{Al}_2\text{O}_3@\text{Ni}/\text{Fe}$ composite, reciprocating circular motion tests for $\text{Al}_2\text{O}_3@\text{Ni}/\text{Fe}$ composites were carried out using a pin-disk friction and wear tester. The friction pair adopted Si_3N_4 with a diameter of 5 mm, and the friction rate was 200 r/min; the load was 20 N, the wear mark diameter was 8 mm, and the time was 3600 s.

2 Results and Discussion

2.1 Characteristics of Ni-encapsulated Al_2O_3 particles

A tightly bonded nickel coating on Al_2O_3 is the premise for preparing $\text{Al}_2\text{O}_3@\text{Ni}/\text{Fe}$ composites. So it is necessary to study the quality of Ni on the surface of Al_2O_3 for improving the interfacial bonding strength of composites. Because it is difficult to accurately characterize due to the limitation in shape and size of Al_2O_3 particles, we used Al_2O_3 plate to do the same experiment to complete the characterization analysis instead of Al_2O_3 particle, and the size of Al_2O_3 plate was 12 mm×18 mm×2 mm. After electroless plating was conducted on Al_2O_3 using the parameters in Table 2 and Table 3, $\text{Al}_2\text{O}_3@\text{Ni}$ plate was obtained. The plate was hung with a string and suspended in solution to make operation easy, so the area around the hole was not observed.

The specimen of $\text{Al}_2\text{O}_3@\text{Ni}$ prepared by ionic liquid assisted electroless plating and the OM micrograph are presented in Fig. 1. From Fig. 1a, Ni coatings covers the surface of Al_2O_3 uniformly and smoothly with no burr and crack. It is speculated that the deposition of Ni coatings begins in pits and holes on the surface of Al_2O_3 and then gradually extends outward. The thickness of Ni coatings is 100.55 μm which is closely bonded to the Al_2O_3 plate (Fig. 1b), which meets the realization of promoting interface reaction and improving interface wettability during next sintering. The morphology of Ni coatings was observed by SEM, as shown in Fig. 2 and Fig. 3. It can be seen that the spore of Ni coatings

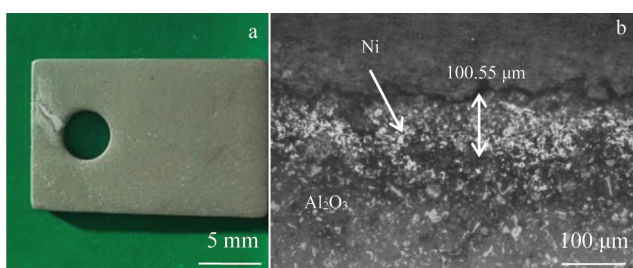


Fig.1 Macrograph (a) and OM image (b) of $\text{Al}_2\text{O}_3@\text{Ni}$ plate prepared by electroless plating

presents a typical cauliflower structure^[14], which means that the Ni coating is amorphous, and the size of Ni spores is 1~4 μm (Fig. 2), indicating that the Ni coating has stable structure, and does not fall off. This compact structure completely covers the Al_2O_3 matrix. Fig. 3 shows a cauliflower Ni, and the mapping result demonstrates that the Ni is distributed uniformly without aggregation. Finally the dense sedimentary Ni layers are obtained.

The coating obtained is Ni-P coating, and the particular reason for this circumstance is the reducing agent (NaH_2PO_2). Therefore, the element P appears in the coating. The element P increases the hardness of coating, but decreases the bonding with substrate. The bonding strength between the coating and substrate is sufficient while the content of P in the coating is 9%~14%^[15]. Therefore, we selected five regions on the coating to calculate the content of P. As shown in Table 4, the content of P in the coating is about 10.5%, which indicates that the element P has no adverse effects on the interface.

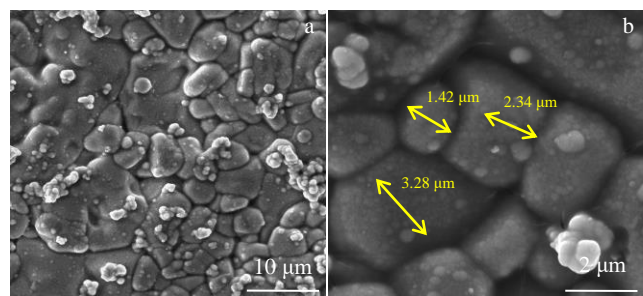


Fig.2 SEM morphologies of $\text{Al}_2\text{O}_3@\text{Ni}$ plate prepared by electroless plating

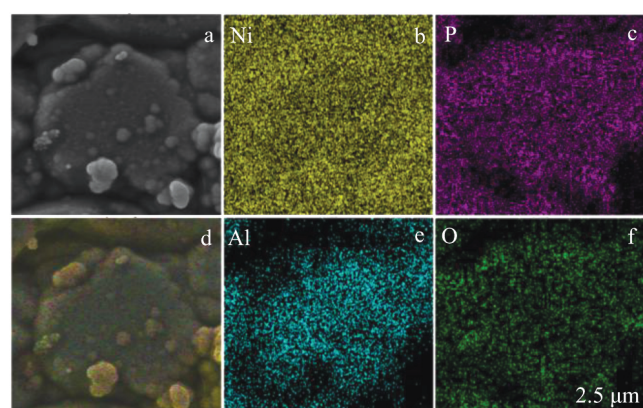


Fig.3 SEM images of $\text{Al}_2\text{O}_3@\text{Ni}$ plate prepared by electroless plating (a, d) and corresponding EDS mappings of Ni (b), P (c), Al (e), and O (f)

Table 4 Chemical composition of coating fabricated by electroless plating (wt%)

Element	1	2	3	4	5	Average
Ni	87.9	90.28	90.8	89.8	88.6	89.5
P	12.1	9.72	9.2	10.2	11.4	10.5

2.2 Interaction mechanism of $\text{Al}_2\text{O}_3\text{p}@\text{Ni}/\text{Fe}$ composites

The same electroless plating process was applied to Al_2O_3 particles, and Ni coated Al_2O_3 particles ($\text{Al}_2\text{O}_3\text{p}@\text{Ni}$) was obtained. The surface morphology of $\text{Al}_2\text{O}_3\text{p}@\text{Ni}$ was observed by SEM, as shown in Fig. 4. There are continuous and compact Ni coatings on the surface of Al_2O_3 particles, and the Ni coatings have cauliflower structure, which is similar to Ni coatings on Al_2O_3 plate (Fig. 2). The EDS mappings of Ni coatings on Al_2O_3 particles are shown in Fig. 5, which demonstrates that the Ni coatings are distributed uniformly and densely.

We mixed $\text{Al}_2\text{O}_3\text{p}@\text{Ni}$ with iron powders at a volume ratio of 1:5, and the mixture was sintered by SPS. $\text{Al}_2\text{O}_3\text{p}@\text{Ni}/\text{Fe}$ composites are obtained (Fig. 6), and $\text{Al}_2\text{O}_3\text{p}@\text{Ni}$ is distributed uniformly in the iron matrix.

The bonding quantity of Al_2O_3 particles and iron matrix will affect the wear resistance of the composites directly, so it is significant to observe the microstructure of interface between Al_2O_3 and iron matrix. The OM micrograph of interface between Al_2O_3 and iron matrix is presented in Fig. 7, and about 60 μm of diffusion layer is observed at the interface. Take a further research by SEM in Fig. 8, it can be seen that at the interface, Ni and Al spread to the side of iron matrix, while Cr

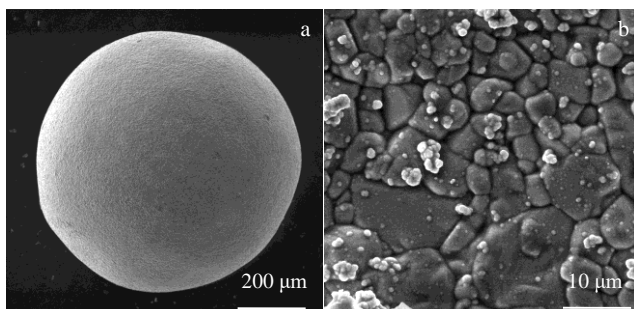


Fig.4 SEM micrographs of $\text{Al}_2\text{O}_3@\text{Ni}$ particles prepared by electroless plating

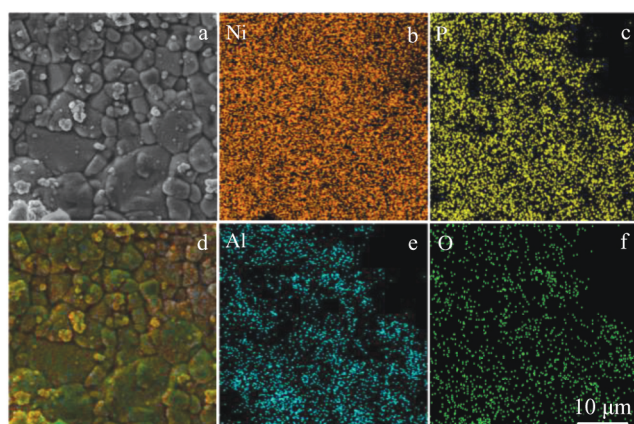


Fig.5 SEM images of $\text{Al}_2\text{O}_3@\text{Ni}$ particles prepared by electroless plating (a, d) and corresponding EDS mappings of Ni (b), P (c), Al (e), and O (f)



Fig.6 Macrograph of $\text{Al}_2\text{O}_3\text{p}@\text{Ni}/\text{Fe}$ composites fabricated by SPS

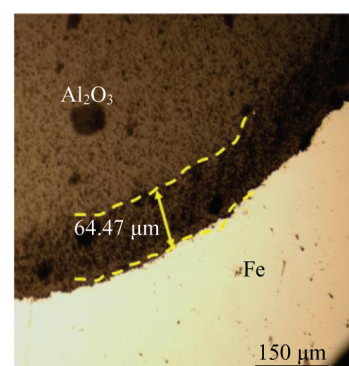


Fig.7 OM micrograph of $\text{Al}_2\text{O}_3\text{p}@\text{Ni}/\text{Fe}$ composites fabricated by SPS

diffuses to the side of Al_2O_3 .

Fig. 9 shows the XRD patterns of interface products of $\text{Al}_2\text{O}_3\text{p}@\text{Ni}/\text{Fe}$ composite and $\text{Al}_2\text{O}_3\text{p}/\text{Fe}$ composite, which demonstrates that there are not only $(\text{Al}_{0.8}\text{Cr}_{0.2})_2\text{O}_3$ but also FeNi_3 and NiAl_2O_4 at the interface.

Based on SEM-EDS mapping (Fig. 8) and XRD results (Fig. 9), the combined mechanism of interface of $\text{Al}_2\text{O}_3\text{p}@\text{Ni}/\text{Fe}$ composites is analyzed as follows. During sintering, Ni coatings diffuse into iron matrix and form infinitude solid solution because of the same fcc crystal structure, which facilitates the diffusion of some elements in Al_2O_3 and iron matrix, and there are $(\text{Al}_{0.8}\text{Cr}_{0.2})_2\text{O}_3$, FeNi_3 and NiAl_2O_4 in the interface, which can be wetted easily with Fe to achieve good wettability at the $\text{Al}_2\text{O}_3/(\text{Al}_{0.8}\text{Cr}_{0.2})_2\text{O}_3/\text{NiAl}_2\text{O}_4/\text{FeNi}_3/\text{Fe}$ interface.

The schematic illustration of combined mechanism of interface of $\text{Al}_2\text{O}_3\text{p}@\text{Ni}/\text{Fe}$ composites is demonstrated in Fig. 10. At the initial stage, the iron is in contact with Al_2O_3 melts, and when Ni is coated on Al_2O_3 contacts with molten iron, they will become soft and migrate into iron matrix (Fig. 10a) and the empty surface of Al_2O_3 is occupied by iron under high pressure of SPS. Meanwhile, metallic Ni has the same crystal structure with austenitic Fe, so it is easy to form infinitude solid solution with Fe. This is in favor of the interdiffusion of Ni and alloying elements between Al_2O_3 surface and iron matrix during the sintering process, so the

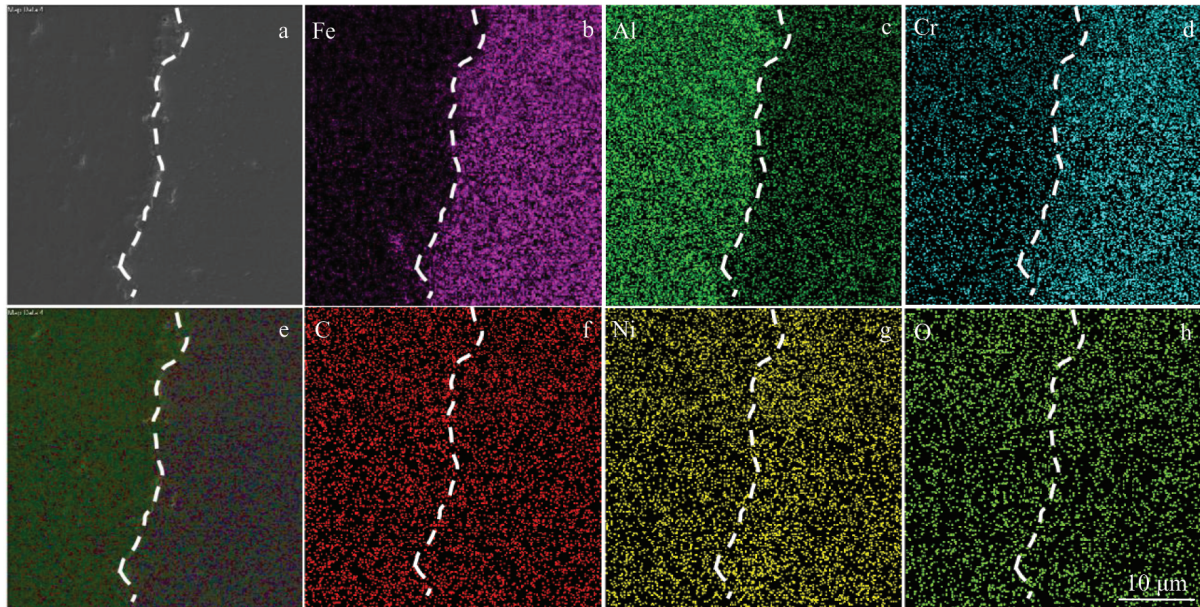


Fig.8 SEM images of $\text{Al}_2\text{O}_3\text{p}$ @Ni/Fe composites fabricated by SPS (a, e) and corresponding EDS mappings of Fe (b), Al (c), Cr (d), C (f), Ni (g) and O (h)

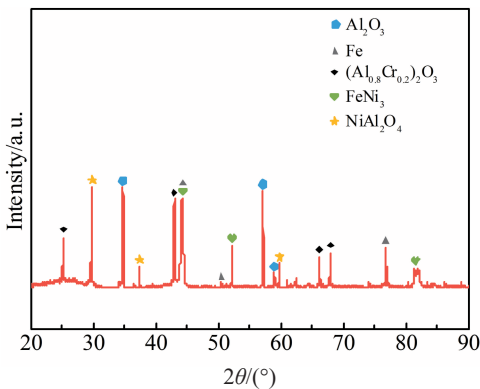


Fig.9 XRD pattern of $\text{Al}_2\text{O}_3\text{p}$ @Ni/Fe composites and $\text{Al}_2\text{O}_3\text{p}$ /Fe composites fabricated by SPS

wettability of ceramic and matrix can be improved (Fig.10b). In addition, the element Cr diffuses into Al_2O_3 and forms $(\text{Al}_{0.8}\text{Cr}_{0.2})_2\text{O}_3$, and a small amount of NiAl_2O_4 and NiFe_3 may form at the interface of Al_2O_3 and iron matrix, which forms a $\text{Al}_2\text{O}_3/(\text{Al}_{0.8}\text{Cr}_{0.2})_2\text{O}_3/\text{NiAl}_2\text{O}_4/\text{FeNi}_3/\text{Fe}$ interface (Fig.10c). The reinforced interface of $\text{Al}_2\text{O}_3\text{p}$ @Ni/Fe is constructed through mechanical bonding, interdiffusion of elements and chemical reactions.

2.3 Friction mechanism of $\text{Al}_2\text{O}_3\text{p}$ @Ni/Fe composites

The effects of Ni coating on wear properties of $\text{Al}_2\text{O}_3\text{p}$ @Ni/Fe composites were investigated by abrasion test under dry friction conditions. The friction mechanism of $\text{Al}_2\text{O}_3\text{p}$ @Ni/Fe composites is further studied. The modified formula of friction coefficient is as follows^[16]:

$$f = \frac{\tau_f}{\sigma} \quad (1)$$

where f is friction coefficient, τ_f is ultimate shear strength, σ is normal compressive stress.

As shown in Fig.11, the curve shows the fluctuation of friction coefficient over time for the two samples. In the initial stage, the friction coefficient increases, which is due to the bare Al_2O_3 particles on the surface of composites. The high hardness of Al_2O_3 particles makes ultimate shear strength τ_f higher to overcome during the friction, which results in an increase in the friction coefficient, and then the curves tend to be stable. In the stable stage, the friction coefficient of $\text{Al}_2\text{O}_3\text{p}$ @Ni/Fe composites is lower than that of $\text{Al}_2\text{O}_3\text{p}$ /Fe composites. Ni coating diffuses into iron matrix in sintering, and the matrix metal near the interface is alloyed to form ferronickel^[17]. The ductility at the interface is improved. Under the action of cyclic loading, the abrasive particles fill into the groove and void to form a solid lubrication layer, thus reducing the friction coefficient. At the same time, Ni coating improves the interface bonding strength between Al_2O_3 and iron matrix, making Al_2O_3 particles difficult to flake off. Therefore, Ni plating treatment on the surface of Al_2O_3 improves the wear resistance.

The stable friction coefficient and mass loss of $\text{Al}_2\text{O}_3\text{p}$ @Ni/Fe and $\text{Al}_2\text{O}_3\text{p}$ /Fe composites are shown in Fig.12. The results demonstrate that $\text{Al}_2\text{O}_3\text{p}$ @Ni/Fe composites have less abrasion mass loss than $\text{Al}_2\text{O}_3\text{p}$ /Fe composites, and $\text{Al}_2\text{O}_3\text{p}$ @Ni/Fe composites have lower friction coefficient, indicating that $\text{Al}_2\text{O}_3\text{p}$ @Ni/Fe composites have smoother friction surface and smaller roughness, which is conducive to resistance to abrasion, so the wear resistance of $\text{Al}_2\text{O}_3\text{p}$ @Ni/Fe composites is relatively better, which means that the layer of Ni has a more positive effect on wear resistance.

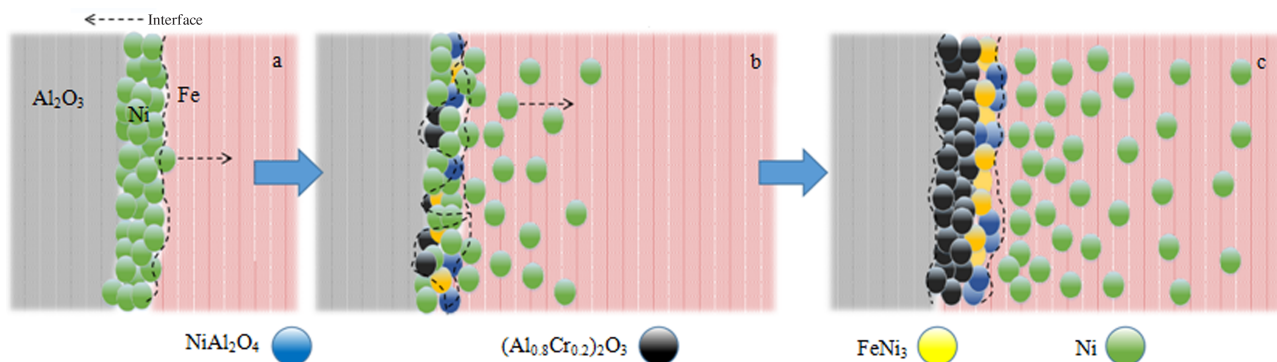


Fig.10 Schematic diagrams of interface connection mechanism of $\text{Al}_2\text{O}_3\text{p}@\text{Ni}/\text{Fe}$ composites: (a) initial stage, (b) reaction stage, and (c) end stage

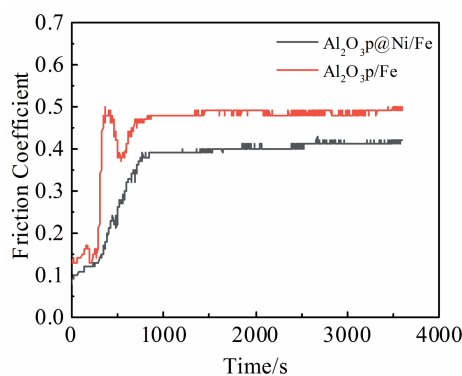


Fig.11 Friction coefficient of $\text{Al}_2\text{O}_3\text{p}@\text{Ni}/\text{Fe}$ composites and $\text{Al}_2\text{O}_3\text{p}/\text{Fe}$ composites

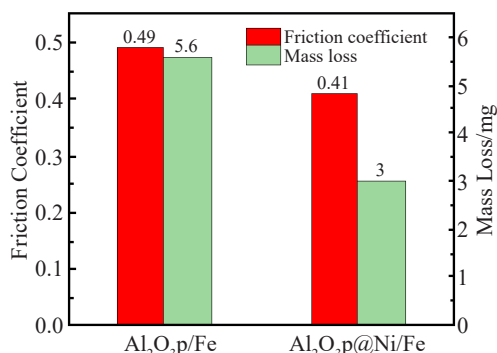


Fig.12 Friction coefficient and mass loss of $\text{Al}_2\text{O}_3\text{p}@\text{Ni}/\text{Fe}$ and $\text{Al}_2\text{O}_3\text{p}/\text{Fe}$ composites

3 Conclusions

- 1) $\text{Al}_2\text{O}_3@\text{Ni}$ particles are prepared by electroless plating. The Ni coatings present a typical cauliflower structure, and the deposition of Ni coatings begins from the pits and holes on the surface of Al_2O_3 and then gradually extends outwards. Finally, the compact structure completely covers the Al_2O_3 matrix.
- 2) $\text{Al}_2\text{O}_3\text{p}@\text{Ni}/\text{Fe}$ composites are prepared by SPS. The Ni

coating improves the wettability of Al_2O_3 particles and Fe. The interface layer of $\text{Al}_2\text{O}_3/(\text{Al}_{0.8}\text{Cr}_{0.2})_2\text{O}_3/\text{NiAl}_2\text{O}_4/\text{NiFe}_2\text{O}_4/\text{Ni}/\text{Fe}$ is formed by mechanical bonding, interdiffusion and chemical reactions, and the interface bonding strength is improved greatly.

3) In the $\text{Al}_2\text{O}_3\text{p}@\text{Ni}/\text{Fe}$ composites, the diffusion of Ni increases the ductility of interface, and a solid lubrication layer forms, thus reducing the attrition. At the same time, Ni coating improves the interface bonding strength between Al_2O_3 and iron matrix, making Al_2O_3 particles difficult to flake off. Therefore, Ni plating treatment on the surface of Al_2O_3 can improve the wear resistance of $\text{Al}_2\text{O}_3\text{p}@\text{Ni}/\text{Fe}$ composites.

References

- 1 Fan Ruirui, Zhang Rui, Li Yan et al. *Material & Heat Treatment* [J], 2011, 40(24): 120 (in Chinese)
- 2 Dang Cong, Liu Huimin, Feng Shan et al. *Rare Metal Materials and Engineering* [J], 2020, 49(12): 4341
- 3 Li Chunyu, Wang Zidong, Li Qingchun et al. *Materials Engineering* [J], 1993(3): 34 (in Chinese)
- 4 Munoz M C, Cerdá J, Beltrán J I et al. *Surface Science Reports* [J], 2006, 61(7): 303
- 5 Hong Haiping, Zhang Wanting, Fan Lei et al. *Ceramics International* [J], 2018, 44(10): 11 013
- 6 Ru Juanjian, He Han, Jiang Yehua et al. *Journal of Alloys and Compounds* [J], 2019, 786: 321
- 7 Ru Juanjian, He Han, Jiang Yehua et al. *Advanced Powder Technology* [J], 2019, 30(10): 2160
- 8 Olgun Ugursoy, Gulfen Mustafa, Gocmez Hasan et al. *Advanced Powder Technology* [J], 2017, 28(9): 2044
- 9 Guo L, Xiao L R, Zhao X J et al. *Ceramics International* [J], 2017, 43(5): 4076
- 10 Wang Hefeng, Shu Xuefeng, Li Xiuyan et al. *Journal of Shenyang University of Technology* [J], 2013, 35(1): 41
- 11 Lu Dongmei, Wang Qingzhou, Zhao Lichen et al. *Rare Metal Materials and Engineering* [J], 2015, 44(5): 1259
- 12 Hillert M. *Alloy Diffusion and Thermodynamics* [M]. Beijing:

Metallurgical Industry Press, 1984: 91

13 Oblack J M, Hehemann R F. *Transformation and Hardenability in Steels*[M]. Michigan: Climax Molybdenum Company, 1967: 5

14 Liu Hong, Qian Daishu. *Transactions of Nonferrous Metals Society of China*[J], 2018, 28(12): 2499

15 Wui Zhen, Liu Jinyun, Du Chunping et al. *Electroplating and Finishing*[J], 2007, 26(5): 20

16 Kukureka Stephen N. *Materials World*[J], 2001, 9(11): 32

17 Zhao Sanfei. *Thesis for Doctorate*[D]. Changsha: Central South University, 2012 (in Chinese)

镍包覆氧化铝增强铁基复合材料的界面行为及其耐磨性

尚方静¹, 王文先¹, 杨 涛², 刘瑞峰³, 周 峻⁴

(1. 太原理工大学 材料科学与工程学院, 山西 太原 030024)

(2. 太原理工大学 机械与运载工程学院, 山西 太原 030024)

(3. 太原理工大学 航空航天学院, 山西 太原 030024)

(4. 宾夕法尼亚州立大学 伊利比伦德学院 机械工程系, 美国 宾夕法尼亚州 16563)

摘要: 采用化学沉积法在 Al_2O_3 表面制备了Ni镀层, 将所制得的Ni包覆 Al_2O_3 颗粒($\text{Al}_2\text{O}_3\text{p@Ni}$)作为铁基体的增强颗粒, 采用SPS法制备了镀镍氧化铝增强铁基复合材料($\text{Al}_2\text{O}_3\text{p@Ni/Fe}$)。通过优化化学镀工艺, 使得 Al_2O_3 表面被Ni层均匀覆盖。Ni镀层呈典型的花椰菜状结构, 尺寸为1~4 μm , 施镀过程中镍首先沉积在 Al_2O_3 表面的凹坑和孔洞中, 然后逐渐长大向外扩展。Ni镀层与 Al_2O_3 紧密结合, 厚度可达100 μm 。在烧结过程中, Ni镀层不仅提高了 Al_2O_3 与铁基体之间的润湿性, 而且促进了 Al_2O_3 与铁基体在界面处的扩散和反应。最终, 通过机械结合、扩散反应和冶金反应形成了 $\text{Al}_2\text{O}_3/\text{NiAl}_2\text{O}_4/(\text{Al}_{0.8}\text{Cr}_{0.2})_2\text{O}_3/\text{NiFe}_2\text{O}_4/\text{Ni}$ 铁基体界面, 大大提高了界面结合强度。同时, 对 $\text{Al}_2\text{O}_3\text{p@Ni/Fe}$ 复合材料和无表面处理的 $\text{Al}_2\text{O}_3\text{p/Fe}$ 复合材料进行了磨损试验, 结果表明, 与 $\text{Al}_2\text{O}_3\text{p/Fe}$ 复合材料相比, $\text{Al}_2\text{O}_3\text{p@Ni/Fe}$ 复合材料的磨损质量损失降低了50%, 摩擦系数降低了12.5%。 $\text{Al}_2\text{O}_3\text{p@Ni/Fe}$ 复合材料的耐磨性明显提高。

关键词: 化学镀; $\text{Al}_2\text{O}_3\text{p@Ni/Fe}$ 复合材料; 放电等离子烧结; 摩擦磨损

作者简介: 尚方静, 女, 1995年生, 硕士, 太原理工大学材料科学与工程学院, 山西 太原 030024, 电话: 0351-6010076, E-mail: 1160734685@qq.com